

Conformational Transitions of Nongrafted Polymers near an Adsorbing Substrate

Michael Bachmann* and Wolfhard Janke†

*Institut für Theoretische Physik, Universität Leipzig, Augustusplatz 10/11, D-04109 Leipzig, Germany**

(Received 4 February 2005; published 29 July 2005)

We have performed multicanonical chain-growth simulations of a polymer interacting with an adsorbing surface. The polymer, which is not explicitly anchored at the surface, experiences a hierarchy of phase transitions between conformations binding and nonbinding with the substrate. We discuss the phase diagram in the temperature-solubility plane and highlight the transition path through the free-energy landscape.

DOI: [10.1103/PhysRevLett.95.058102](https://doi.org/10.1103/PhysRevLett.95.058102)

PACS numbers: 87.15.Aa, 05.10.-a, 87.15.Cc

The recent developments in single molecule experiments at the nanometer scale, e.g., by means of atomic force microscopy (AFM) [1] and optical tweezers [2], now allow for a more detailed exploration of structural properties of polymers in the vicinity of adsorbing substrates [3]. The possibility to perform such studies is of essential biological and technological significance. From the biological point of view the understanding of the binding and docking mechanisms of proteins at cell membranes is important for the reconstruction of biological cell processes. Similarly, specificity of peptides and binding affinity to selected substrates could be of great importance for future electronic nanoscale circuits and pattern recognition nanosensory devices [4]. The study of models similar to the one considered in this work has considerable applications for a broad variety of problems, e.g., understanding the mechanisms of protein-ligand binding [5], prewetting and layering transitions in polymer solutions as well as dewetting of polymer films [6], molecular pattern recognition [7], and electrophoretic polymer deposition and growth [8].

In computer simulations and analytical approaches, typically, one end of the polymer is anchored at a flat substrate and the influence of adhesion and steric hindrance [9–14], pulling forces [15,16], or external fields [17] on the shape of the polymer is considered. The question of how a flexible substrate, e.g., a cell membrane, bends as a reaction of a grafted polymer, was addressed, for example, in Ref. [18]. Proteins exhibit a strong specificity as the affinity of peptides to adsorb at surfaces depends on the amino acid sequence, solvent properties, and substrate shape. This was experimentally and numerically studied, e.g., for peptide-metal [19,20] and peptide-semiconductor [21,22] interfaces. The binding-folding and docking properties of lattice heteropolymers at an adsorbing surface were the subject of a recent numerical study [23].

In this work we investigate in detail the temperature and solubility dependence of adsorption properties for a polymer which is *not fixed* at the surface of the substrate with one of its ends. This model was inspired by the experimental setup used in Refs. [21,22], where the peptides are initially freely moving in solution before adsorption. Therefore, there are two main differences in comparison

with studies of polymers explicitly grafted at the substrate: First, the chain can completely desorb from the substrate, allowing for the investigation of the binding-unbinding transition. Second, adsorbed conformations are possible where none of the two polymer ends are in contact with the surface.

For our study, we use a simple lattice model [10], where the energy for a polymer near an adsorbing substrate is given by $E_s(n_s, n_m) = -n_s - sn_m$ (in natural units). Therein, $n_{s,m}$ are the numbers of nearest-neighbor monomer-surface and monomer-monomer contacts, respectively. The solvent parameter s takes account of the goodness of the implicit solvent (the smaller the s , the better the solvent) and rates the two energy scales. The partition sum per surface area A is (with $k_B \equiv 1$)

$$Z(T, s)/A = \sum_{n_s, n_m} g_{n_s, n_m} e^{-E_s(n_s, n_m)/T}, \quad (1)$$

where g_{n_s, n_m} is the contact density. Since the number of unbound conformations in the half-space accessible to the polymer is unrestricted, g_{n_s, n_m} formally diverges for $n_s = 0$. For regularization, we introduce an impenetrable (but neutral, i.e., nonadhesive) wall at a sufficiently large distance z_w from the substrate, in order to keep its influence on the unbound polymer small.

We generalized the powerful multicanonical chain-growth algorithm, originally introduced for the simulation of lattice proteins [24], in order to simulate the contact density g_{n_s, n_m} directly. This algorithm, which sets up on the pruned-enriched Rosenbluth method (PERM) [25], enables an optimal sampling of the contact space, and all energetic quantities such as, e.g., the specific heat are obtained by reweighting the density of contacts with respect to temperature and solubility. The main advantage is that the whole phase diagram can, in principle, be constructed within a *single* simulation [26]. This method is the key for unravelling the detailed structure of the phase diagram, in particular, at low temperatures, where most Monte Carlo algorithms based on importance sampling run into difficulties. In order to break correlations being inherent in the chain-growth process, we averaged over independent simulations, and a total statistics of more than 10^9 chains

was accumulated in the production runs for a homopolymer with 100 monomers. For confirmation, we also investigated polymers with up to 200 monomers [27].

In Fig. 1 we show the pseudophase diagram of the 100-mer near an attractive substrate and the steric wall in a distance $z_w = 200$ from the substrate. The color codes the height of the specific heat C_V as a function of temperature T and solvent parameter s ; the brighter the color, the larger the value of C_V . The white and black lines emphasize the maxima of the specific heat, which shall serve as an orientation for the phase boundaries. While the white lines indicate pseudotransitions specific for the 100-mer, lines drawn in black separate regions which are expected to be phases in the strict thermodynamic sense. The precise locations of transition lines in the thermodynamic limit $N \rightarrow \infty$ will, however, differ from the position for the finite-length system under study. We distinguish six thermodynamic phases, four for the adsorbed (AC1, AC2, AE1, and AE2) and two for the desorbed (DC and DE) polymer [28]. In the adsorbed-collapsed phase AC1, all monomers are in contact with the substrate and the two-dimensional (single-layer) conformation (“film”) is very compact. The transition from AC1 to AC2 is the layering phase transition from single- to double-layer conformations. The white transition lines within AC2 indicate pseudotransitions to compact conformations with more than two layers. These transitions are expected to disappear in the thermodynamic limit [13]. The transition line between AC1 and the adsorbed-expanded phase AE1 is the two-dimensional Θ collapse. It separates the compact single-layered conformations in AC1 from the dissolved, but still basically two-dimensional, conformations. The white lines in AE1 indicate conformational transitions to unstructured conformations extending partially into the third dimension. The substrate-contacting layer is dissolved and although

several layers can form, no explicit layering transitions are observed in this region. In contrast to AE1, the conformations dominating phase AE2 possess a very compact surface layer but less compact upper layers. As in AE1, the formation of higher-order layers is not accompanied by noticeable conformational transitions. The difference between AE1 and AE2 becomes more apparent when approaching the unbinding transition line to phases DE and DC, where the polymer has completely desorbed from the substrate: In the desorbed-expanded phase DE random-coil conformations dominate, while in the desorbed-collapsed phase DC globular conformations are favored. Phases DE and DC are separated by the transition line indicating the three-dimensional Θ collapse. This transition line, together with the transition lines AC1/AE1 and AE2/AE1, is parametrized by $s_0(T)$, which separates *poor* ($s > s_0$) from *good* ($s < s_0$) solvent. This quite complex phase diagram has been further supported by our analyses of structural quantities such as the gyration tensor of the polymer chain, e.g., by its strong anisotropy in the transition between phases AC1 and AE1, reflecting the dominating filmlike conformations. At the collapse transition DC/DE, we observe, as expected, isotropic behavior [27].

The main difference in comparison to a polymer that is *explicitly* anchored at the substrate with one of its ends is the occurrence of the strong binding-unbinding transition between the A and D phases. In the D phases, the polymer can move freely within the cavity, restricted only by the presence of the two impenetrable walls. However, this transition also influences the conformational behavior of the polymer in phases AE1 and AE2, the latter not being present for the anchored polymer. In fact, phases AC2, AE2, and DC lie within the DC/SAG (surface-attached globule) regime of the anchored polymer [11,13], whose precise phase structure is not yet completely clarified. Phases AE1, AC1, and AC2 approximately coincide in the two systems for low temperatures, although the system in our study has more entropic freedom since adsorbed conformations are also possible, where none of the two ends are anchored at the substrate. This may have consequences for the location of transition lines.

Apart from the thermodynamic transitions in the traditional meaning, we also see pseudotransitions being specific to the chosen number of monomers (e.g., a reorientation transition from the $5 \times 5 \times 4$ cube with 25 surface contacts to the rotated cube exhibiting only 20 contacts with the substrate, which occurs within phase AC2 at $T \approx 0.7$) [27]. We are convinced that growing experimental capabilities will allow the observation of these effects also for short synthetic or naturally occurring polymers (e.g., peptides).

Thermodynamically, the conformations dominating a certain phase correspond to the minimum of a suitably coarse-grained free energy depending on a few characteristic observables of the system. The complexity of the free-energy landscape and its dependence on external parameters such as temperature or solvent strongly influence the

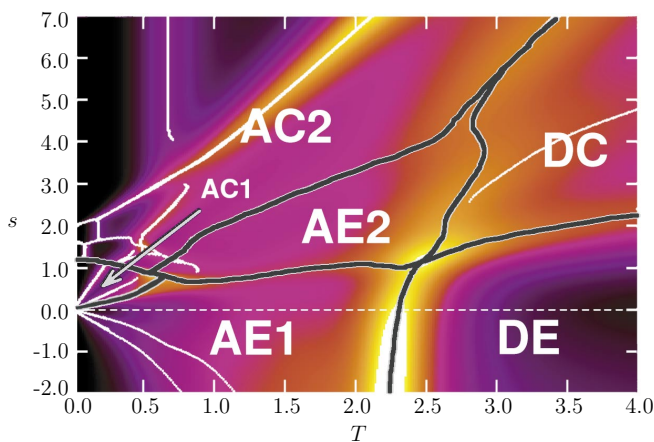


FIG. 1 (color online). Pseudophase diagram of a polymer with 100 monomers obtained from the specific heat C_V as a function of temperature T and solubility parameter s . The white and black drawn lines indicate the ridges of the specific heat profile (see text). The dashed line separates the regions of attractive and repulsive monomer-monomer interaction.

kinetics of phase transitions. For the polymer near an adsorbing surface, we choose the numbers of monomer-substrate contacts, n_s , and those between monomers, n_m , as system observables. According to Eq. (1), the probability for a polymer conformation is given by $p(n_s, n_m) \propto g_{n_s, n_m} \exp([n_s + sn_m]/T)$ and the contact free energy reads as $F_{s,T}(n_s, n_m) = -T \ln p(n_s, n_m)$, where the temperature T and the solubility s are fixed external parameters.

In Fig. 2 we have included all minima of the contact free energy for the parameter set $T \in [0, 4.0]$, $s \in [-2.0, 4.0]$. Given a fixed solubility s , the stability of a conformation with minimal free energy is connected with the range of temperatures ΔT over which the associated free energy is actually the global free-energy minimum. We have included in Fig. 2, for several fixed solubilities, the “paths” of free-energy minima hit when increasing the temperature from $T = 0$ up to $T = 4$, which is moving from right to left.

As an example, we consider the case $s = 1$ for the whole region of temperatures. In Table I we have listed the conformational transitions the 100-mer experiences by increasing the temperature and depicted typical conformations for each phase. We start at $T = 0$ with the ground state which is formed by lamellar maximally compact two-dimensional conformations with 100 surface contacts and 81 monomer-monomer contacts. It is highly degenerate and, in fact, realized by about 10^{14} (including all symmetries except translation) different conformations. The ground state remains stable until $T \approx 0.2$, where the structures become less ordered. The lamellar structure is dissolved, but all in all they are still two dimensional and very compact. The conformational changes in the transition from I to II are rather local, in contrast to the probably actual phase transition from II to III at $T \approx 0.5$, where the number of surface contacts is drastically reduced to about half the value of the ground-state conformation and thus a

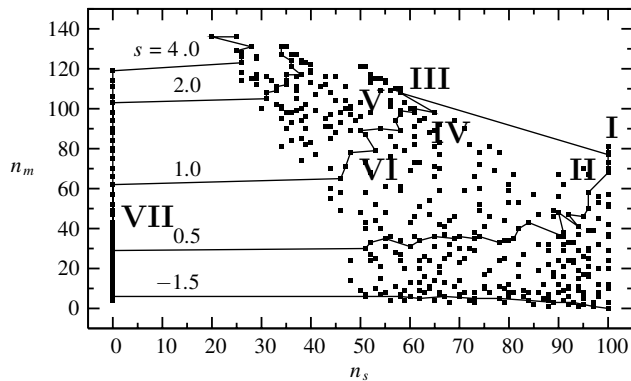


FIG. 2. Map of free-energy minima identified in the space of contact numbers n_s with the substrate and n_m between monomers. Also shown are exemplified paths through the free-energy landscape for different fixed solvent parameters s . The labels I to VII refer to the pseudophases in the case $s = 1$, described in detail in the text and in Table I. The lines are guides to the eye only.

second layer forms. In Fig. 2 this transition appears as a jump from the surface state $(n_s, n_m) = (100, 77)$ to $(58, 108)$. As can be seen in Fig. 3, the probability distribution $p(n_s, n_m)$ exhibits two distinct peaks at this temperature, which is interpreted as a strong signal for a first-order transition. Entering regime IV, i.e., the adsorbed-expanded phase AE2, the dissolution of the surface-contacting layer begins. This process continues after passing the pseudo-transition line to section V, where higher-order layers form. Respective surface layer and upper layers still form connected parts, in contrast to phase VI (which belongs to AE1), where upper layers can break apart and form isolated islands. Increasing the temperature further, we approach the second strong first-order-like transition line and the polymer unbinds from the substrate for temperatures

TABLE I. “Path” through the landscape of free-energy minima for a 100-mer in solvent with solubility $s = 1$ with increasing temperature. Monomers in contact with the adsorbing substrate are shaded in light gray.

Phase	T	n_s	n_m	Typical conformations	
AC1	I	0.0–0.2	100	81	
	II	0.2–0.5	100	77 ± 1	
AC2	III	0.5–0.6	58	108	
AE2	IV	0.6–1.1	61 ± 4	95 ± 5	
	V	1.1–1.4	53 ± 2	88 ± 2	
AE1	VI	1.4–2.2	50 ± 4	71 ± 7	
DE	VII	2.2– ∞	0	≤ 62	

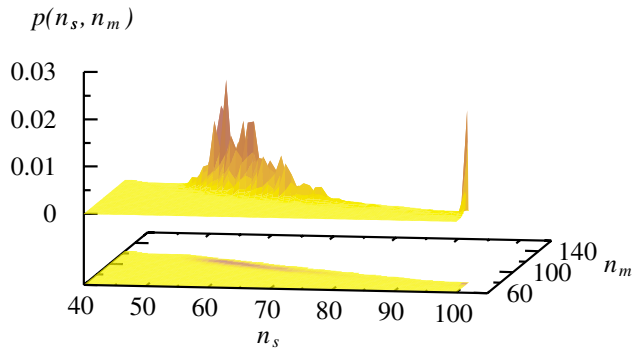


FIG. 3 (color online). Probability distribution $p(n_s, n_m)$ for the 100-mer in solvent with $s = 1$ at $T = 0.49$, where the polymer experiences the layering transition from a single to a double layer.

$T > 2.2$. The free-energy minimum jumps from the contact state (46, 65) to (0, 62) discontinuously (again, see Fig. 2). Therefore, the conformations occurring in phase VII do not longer prefer surface contact. Since the thermal energy superimposes the relatively weak attraction between the monomers at these temperatures, the 100-mer in solvent with $s = 1$ does not experience the three-dimensional Θ transition, because it is already in the random-coil phase after the unbinding. Note that we have also missed the two-dimensional Θ collapse on the substrate. For this to happen, the quality of the solvent would have to be better (i.e., smaller values of s). From the free-energy perspective, both collapse transitions are of second order, since the free-energy minima of the 100-mer at $(n_s, 100)$ (two-dimensional surface-layer conformations) and $(0, n_m)$ (three-dimensional conformations without contact to the surface) change continuously for increasing temperature (see Fig. 2).

In this work, by analyzing the global minima in the free-energy landscape, we have qualitatively determined the complete T - s phase diagram for a polymer with 100 monomers in solvent near an adsorbing substrate. Two types of conformational transitions are experienced by the polymer, phase transitions in the thermodynamic sense and transition-type crossover effects which are specific to the given finite number of monomers. In the first case, further simulations of longer polymers combined with finite-size scaling analyses will give more precise estimates for the associated transition lines. Physically perhaps even more interesting, however, are the geometrically induced crossover effects which are expected to become more and more important as the high-resolution experimental equipment allows concrete measurements in the nanometer range, and the design of nanoscale devices will take advantage of the specific properties of finite-length polymers.

We thank Karsten Goede and Marius Grundmann for interesting discussions on peptide adsorption at semiconductor surfaces. This work is partially supported by the German-Israel Foundation (GIF) under Grant No. I-653-181.14/1999.

*Electronic address: Michael.Bachmann@itp.uni-leipzig.de

†Electronic address: Wolfhard.Janke@itp.uni-leipzig.de

‡Electronic address: <http://www.physik.uni-leipzig.de/CQT>

- [1] M. Rief, H. Clausen-Schaumann, and H. Gaub, *Nat. Struct. Biol.* **6**, 346 (1999).
- [2] D. E. Smith, S. Tans, S. Smith, S. Grimes, D. L. Anderson, and C. Bustamante, *Nature (London)* **413**, 748 (2001).
- [3] J. J. Gray, *Curr. Opin. Struct. Biol.* **14**, 110 (2004).
- [4] E. Nakata, T. Nagase, S. Shinkai, and I. Hamachi, *J. Am. Chem. Soc.* **126**, 490 (2004).
- [5] E. Balog, T. Becker, M. Oettl, R. Lechner, R. Daniel, J. Finney, and J. C. Smith, *Phys. Rev. Lett.* **93**, 028103 (2004); M. Ikeguchi, J. Ueno, M. Sato, and A. Kidera, *Phys. Rev. Lett.* **94**, 078102 (2005).
- [6] J. Forsman and C. E. Woodward, *Phys. Rev. Lett.* **94**, 118301 (2005); G. Reiter, *Phys. Rev. Lett.* **87**, 186101 (2001).
- [7] T. Bogner, A. Degenhard, and F. Schmid, *Phys. Rev. Lett.* **93**, 268108 (2004).
- [8] G. M. Foo and R. B. Pandey, *Phys. Rev. Lett.* **80**, 3767 (1998); *Phys. Rev. E* **61**, 1793 (2000).
- [9] R. Hegger and P. Grassberger, *J. Phys. A* **27**, 4069 (1994).
- [10] T. Vrbová and S. G. Whittington, *J. Phys. A* **29**, 6253 (1996); **31**, 3989 (1998); T. Vrbová and K. Procházka, *J. Phys. A* **32**, 5469 (1999).
- [11] Y. Singh, D. Giri, and S. Kumar, *J. Phys. A* **34**, L67 (2001); R. Rajesh, D. Dhar, D. Giri, S. Kumar, and Y. Singh, *Phys. Rev. E* **65**, 056124 (2002).
- [12] M. S. Causo, *J. Chem. Phys.* **117**, 6789 (2002).
- [13] J. Krawczyk, T. Prellberg, A. L. Owczarek, and A. Rechnitzer, *Europhys. Lett.* **70**, 726 (2005).
- [14] J.-H. Huang and S.-J. Han, *J. Zhejiang Univ. Sci.* **5**, 699 (2004).
- [15] F. Celestini, T. Frisch, and X. Oyharcabal, *Phys. Rev. E* **70**, 012801 (2004).
- [16] J. Krawczyk, T. Prellberg, A. L. Owczarek, and A. Rechnitzer, *J. Stat. Mech.* (2004) P10004.
- [17] P. Benetatos and E. Frey, *Phys. Rev. E* **70**, 051806 (2004).
- [18] M. Breidenreich, R. R. Netz, and R. Lipowsky, *Europhys. Lett.* **49**, 431 (2000); *Eur. Phys. J. E* **5**, 403 (2001).
- [19] S. Brown, *Nat. Biotechnol.* **15**, 269 (1997).
- [20] R. Braun, M. Sarikaya, and K. Schulten, *J. Biomater. Sci., Polym. Ed.* **13**, 747 (2002).
- [21] S. R. Whaley, D. S. English, E. L. Hu, P. F. Barbara, and A. M. Belcher, *Nature (London)* **405**, 665 (2000).
- [22] K. Goede, P. Busch, and M. Grundmann, *Nano Lett.* **4**, 2115 (2004).
- [23] N. Gupta and A. Irbäck, *J. Chem. Phys.* **120**, 3983 (2004).
- [24] M. Bachmann and W. Janke, *Phys. Rev. Lett.* **91**, 208105 (2003); *J. Chem. Phys.* **120**, 6779 (2004).
- [25] P. Grassberger, *Phys. Rev. E* **56**, 3682 (1997).
- [26] For a related method, see T. Prellberg and J. Krawczyk, *Phys. Rev. Lett.* **92**, 120602 (2004).
- [27] M. Bachmann and W. Janke (to be published).
- [28] The intersection of the transition lines near $T \approx 2.5$ splits in fact in two tricritical points, as we know from a preliminary study of polymers with up to 200 monomers [27].